Mesonic Enhancement of the Weak Axial-Vector Current Evaluated from β Decay in the Lead Region

E. K. Warburton
Brookhaven National Laboratory, Upton, New York 11973
(Received 18 January 1991)

A shell-model study is made of first-forbidden β decay in $A=205$–212 nuclei. A least-squares fit for eighteen $\Delta J=0$ and 1 decays gave a scaling factor for the rank-one contributions of 0.97 ± 0.06, i.e., agreement with experiment, and an enhancement factor $\epsilon_{\rm MEC}$ for the rank-zero matrix element of γ_5 of 2.01 ± 0.05, indicating an enhancement by 100% over the impulse approximation. A 40% effect is predicted from meson exchange. Thus, a deficiency in the meson-exchange calculation or some further unforeseen effect is suggested.

PACS numbers: 23.40.Hc, 21.60.Cs, 23.40.Bw, 27.80.+w

A large meson-exchange-current (MEC) contribution to the timelike component of the weak axial-vector current γ_5 in nuclear media was predicted in 1978.[1,2] The enhancement over the impulse approximation is predicted to be $\sim$(40–70)% and insensitive to nuclear structure and details of the MEC.[3,4] It is most easily observed via its effect on first-forbidden β (FFB) decay. Most of the activity generated by this prediction has centered on the $A=16$ region[3,5,6] and theoretical studies are still being carried out there.[7] Evidence for MEC effects has also been found for $A\sim40$ and 96.[8,9] The lead region provides a large number of FFB decays including the fastest known (see Fig. 1). Nevertheless, there has been no detailed MEC studies at $A\sim208$. It is the purpose of this Letter to describe such a study. More detail, including a discussion of specific decays, will be given in a longer article.[11]

The β matrix elements are calculated via

$$M_R^a=\sum_{j_i j_f}\mathcal{M}_R^a(j_i j_f)=\sum_{j_i j_f}D_R(j_i j_f)M_R^a(j_i j_f,\text{eff})$$
$$=\sum_{j_i j_f}D_R(j_i j_f)q_a(j_i j_f)M_R^a(j_i j_f)\,. \qquad (1)$$

In Eq. (1) a labels a matrix element of rank R, $M_R^a(j_i j_f)$ is a single-particle matrix element for the transition $j_i\rightarrow j_f$ in the impulse approximation, and the quenching factor $q_a(j_i j_f)$ corrects $M_R^a(j_i j_f)$ for the finite size of the model space. The $D_R(j_i j_f)$ are the one-body transition densities which are the result of the shell-model calculations performed with the code OXBASH.[12] Calculations for all $A=205$–212 nuclei of Fig. 1 were made with realistic interactions based on G-matrix descriptions of nucleon-nucleon potentials as well as with a surface-δ interaction[13] (SDI). The Kuo-Herling[14,15] interactions for particles (KHP) above and holes (KHH) below ^{208}Pb form the basis of the interaction. In order to incorporate 1p-1h excitations into the calculations performed with the two Kuo-Herling interactions and to calculate the $A=207$–209 decays, an interaction which connects the KHH and KHP model spaces was developed in the model space of Poppelier and Glaudemans.[13] The two KH interactions were truncated (with compensating modifications) to this model space (see Fig. 2).[11,15] The 1p-1h part of the Poppelier-Kuo-Herling (PKH) interaction was generated by a G-matrix potential[16] (H7B) plus the Coulomb potential.

The decay rates were calculated using the full rigor

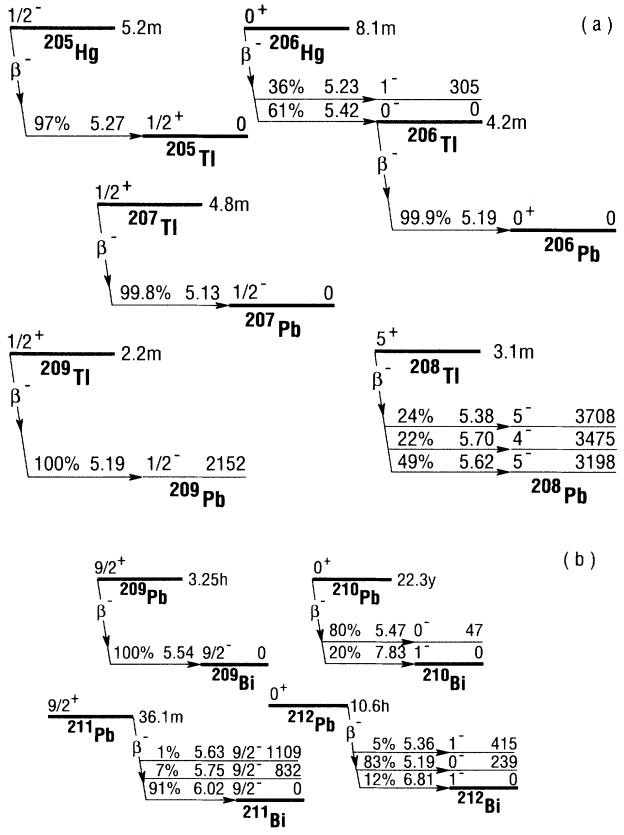

FIG. 1. FFB decays for (a) $A=205$–209 and (b) $A=209$–212. β branches and $\log ft$ values (Ref. 10) are given.

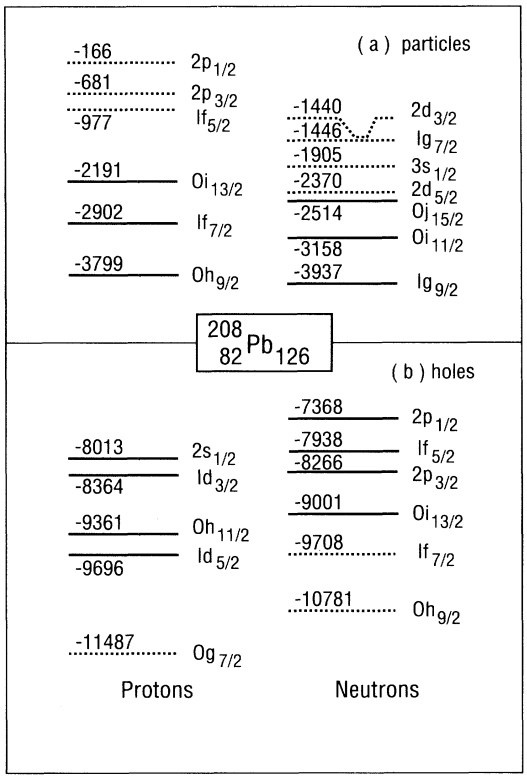

FIG. 2. The Kuo-Herling and PKH model spaces. Single-particle energies (keV) are experimental. The Kuo-Herling interaction includes all the orbits shown and is for either (a) particles above ^{208}Pb or (b) holes below ^{208}Pb. The two are not connected. The PKH model space includes fourteen orbits (solid lines) with the particle and hole orbits connected.

and accuracy of the Behrens-Bühring formalism[17] including consideration of higher-order terms in the expansion of the shape factor and in the evaluation of the Fermi integral.[8,11] To summarize, the rank-zero ($R0$) and rank-one ($R1$) components of FFB decays can be formulated in terms of two $R0$ matrix elements M_0^S and M_0^T —the spacelike and timelike components of the axial-vector current—and two $R1$ matrix elements M_1^x and M_1^u—the $E1$-like and $R1$ spin-dipole operators. The matrix elements $M_R^a(j_i j_f)$ were evaluated using Woods-Saxon wave functions.[18] The dependence on the separation energies of the νj_i and πj_f orbits was examined critically.[11] Contributions from excitations of the core can have a large effect on the first-forbidden matrix elements.[19] The important core-excited admixtures in the initial (final) state are those connected by a one-body operator to the dominant terms in the final (initial) state. Restrictions on the matrix elements of $\mathbf{r}$ and its derivatives limits first-forbidden decay to transitions between adjacent major shells. This selection rule and Pauli blocking severely restricts the contributions from initial-state admixtures. Only those transitions involving $0h_{11/2}$ proton holes contribute and all are included in the PKH model space. There are many possible transitions involving the 2p-2h admixtures in the final state. Those affecting the allowable transitions from the PKH model space were recently considered.[19] These results give explicit values for the $q_a(j_i j_f)$ of Eq. (1) derived using the H7B interaction.

Comparison to experiment is made here via the averaged shape factor[17]

$$\langle C(W)\rangle = 9195\times 10^4/f_0 t = \sum_R B_1^{(R)} = B_1^{(0)} + B_1^{(1)} + B_1^{(2)}\ \mathrm{fm}^2 . \quad (2)$$

The ζ approximation is useful for displaying the physics involved in the $R0$ and $R1$ decays:[8,11]

$$B_1^{(0)} = (M_1^{(0)})^2 = (\epsilon_{\mathrm{MEC}} M_0^T + a_S M_0^S)^2 ,$$
$$B_1^{(1)} = (M_1^{(1)})^2 = (a_u M_1^u - a_x M_1^x)^2 , \quad (3)$$

where the a_a are positive, largely kinematical and insensitive to nuclear structure. The ζ approximation has errors of $\leq 4\%$ for $R0$ and $\leq 10\%$ for $R1$. For harmonic-oscillator wave functions, $M_0^T(j_i j_f)$ and $M_0^S(j_i j_f)$ are related by[8]

$$M_0^T(j_i j_f) = -(E_{\mathrm{osc}}/m_e c^2) M_0^S(j_i j_f) . \quad (4)$$

Using Eq. (4) with $E_{\mathrm{osc}} = \hbar\omega = 7$ MeV and $a_S \approx 14$, we have $B_1^{(0)} \approx (14\epsilon_{\mathrm{MEC}} - 14)^2 (M_0^S)^2$ fm^2. It is clear from this approximation why the observation of fast $R0$ decays calls for strong enhancement. On the average $a_u|M_1^u| \sim a_x|M_1^x|$, so that the $R1$ decay rate depends critically on the relative phase of M_1^u and M_1^x which varies with j_i and j_f. For example, the phase is odd for $\nu 2p_{1/2} \rightarrow \pi 2s_{1/2}$ and even for $\nu 1g_{9/2} \rightarrow \pi 0h_{9/2}$, thus providing a simple explanation for the strong $R1$ contributions to the decays of Fig. 1(a) and the weakness of the ground-state decays in Fig. 1(b).

Results for the D_R included input from either the KHH or KHP interaction, and all 1p-1h excitations across the ^{208}Pb interface with the PKH interaction. For $A = 207$–209 only the PKH calculation is relevant. The J dimensions of the PKH calculations varied up to 2538.

With the $R0$ and $R1$ matrix elements evaluated as described, a least-squares fit was made with

$$\langle C(W)\rangle^{1/2} = [B_1^{(0)}(\epsilon_{\mathrm{MEC}}) + B_1^{(1)}(sq_1)]^{1/2} , \quad (5)$$

where the quantities varied in the fit are explicitly displayed as variables and sq_1 is a state-independent scaling factor for $M_1^{(1)}$. The fit was made to the eighteen decays shown in Fig. 1 and gave $\epsilon_{\mathrm{MEC}} = 2.01 \pm 0.05$, $q_1 = 0.97 \pm 0.06$, and χ_D^2 (χ^2 per degree of freedom) equal to 1.00 if a uniform uncertainty of 13% is ascribed to the calculation of all eighteen $\langle C(W)\rangle^{1/2}$. The results of the fit with Eq. (5) are summarized in Fig. 3. How sensitive is the result to the specific shell-model interaction used? The SDI results for ϵ_{MEC} for all decays of Fig. 1 except those for $A = 208$ (not calculated) were consistent with the result of $\epsilon_{\mathrm{MEC}} = 2.01$ but with a larger spread in indi-

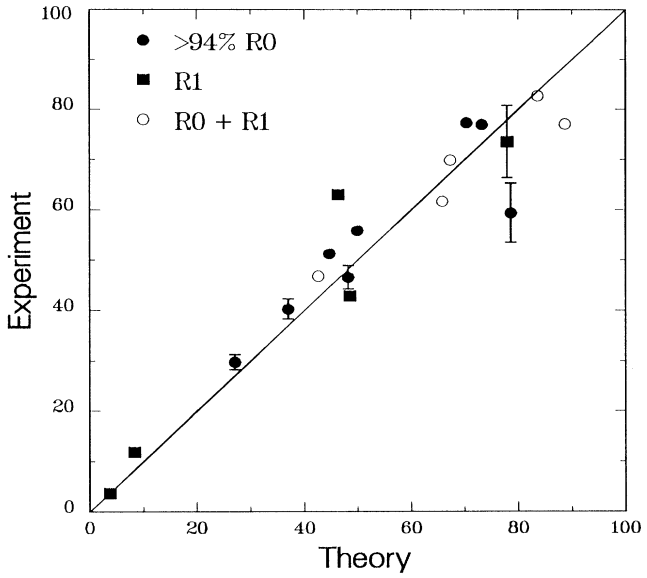

FIG. 3. Comparison of experimental and theoretical values of $\langle C(W)\rangle^{1/2}$ (in fm) for the decays of Fig. 1. Experimental errors are shown only if they exceed the size of the symbols.

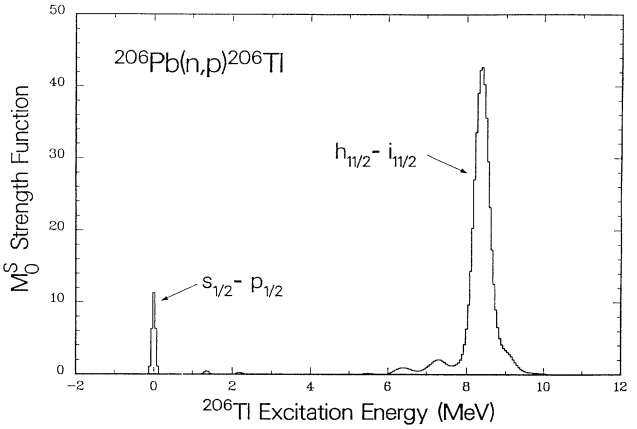

FIG. 4. Strength distribution (matrix element squared) for the $R0$ matrix element M_0^S connecting excited states of ^{206}Tl to the 0^+ ground state of ^{206}Pb. The theoretical distributions have been folded with a Gaussian function for ease of viewing and to simulate the experimental resolution which might pertain for the inverse charge-exchange reaction. The dominant ν-π transition is indicated for the major structures.

vidual values (a least-squares fit was not performed). It is clear that the parametrization of Eq. (5) results in a highly successful description of the decays of Fig. 1.

The eighteen decays show a great deal of regularity and can be understood with simple ideas. To aid this understanding the $R0$ and $R1$ strength distributions for $^{206}\mathrm{Tl}(0^-,1^-)\leftrightarrow{}^{206}\mathrm{Pb}(0_1^+)$ were calculated in the PKH model space with all possible 1p-1h excitations included. The strength distribution for $(M_0^S)^2$ is shown in Fig. 4. The distribution for $(M_0^T)^2$ will be, of course, nearly identical to that of $(M_0^S)^2$, i.e., see Eq. (4); those for the $R1$ decays are similar. As expected, the spectrum of Fig. 4 is dominated by a particle-hole "giant resonance." Recall that other first-order effects have been incorporated via the $q_\alpha(j_i j_f)$ which, in this case, represent the effects of "particle-hole" admixtures in ^{206}Pb and thus would be manifested by a giant resonance in ^{206}Pb if the reverse experiment were performed.

Contributions to the $^{206}\mathrm{Hg}(0^+)\rightarrow{}^{206}\mathrm{Tl}(0_1^-)$ decay shown in Table I display a pronounced coherency. All single-particle transitions are in phase except the $\nu 0i_{11/2}\rightarrow\pi 0h_{11/2}$ particle-hole transition. This behavior is due to the general nature of the interaction; the particle-particle and hole-hole interactions are attractive so that their strength is concentrated in one (or a few) state and pushed to low energy in the same manner and to a comparable degree as the familiar 2_1^+ state in even-even nuclei. Likewise, the particle-hole interaction is repulsive so its strength is concentrated at higher energies and its contribution to lower states will be destructive. With two exceptions, this simple behavior is observed for all the $R0$ contributions of Fig. 3. These exceptions are connected to the concept that the hole-hole plus particle-particle strength is isolated. Let us call this strength a "pygmy" resonance. It is expected that initial states will have a pygmy resonance in the final nucleus as well. The exception to the coherency occurs when the initial and final states are not each others pygmy resonances. Transitions between other states will, of course, not display this strong coherence, and, in fact, can be expected to display a great deal of destructive interference. In some instances we observe a state for which the destructive interference is maximal while the individual single-particle contributions are strong. We term this state "anticoherent."

For the decays of Fig. 3 there are two cases for which the pygmy resonance does not include the lowest-lying state. These are $^{208}\mathrm{Tl}(5^+)\rightarrow{}^{208}\mathrm{Pb}(5_1^-)$ and $^{211}\mathrm{Pb}(\frac{9}{2}^+)\rightarrow{}^{211}\mathrm{Bi}((\frac{9}{2})_1^-)$. In the first case, the (p,n) pygmy resonance of the $^{208}\mathrm{Tl}(5_1^+)$ state is isolated in the $^{208}\mathrm{Pb}(5_2^-)$ state—in the $R0$ decay to the 5_1^- state all

TABLE I. Predicted values for the rank-zero $D_R(j)$ and M_δ^T of Eq. (1) for the decay of $^{206}\mathrm{Hg}(0^+)$ to the first 0^- state of ^{206}Tl. The results for M_δ^S show the same coherence. Note $j_i=j_f\equiv j$ for $R0$ decays.

νj_i	πj_f	$D_0(j)$	$M_\delta^T(j,\mathrm{eff})$	$\mathcal{M}_\delta^T(j)$
$f_{7/2}$	$g_{7/2}$	0.002	165.813	0.347
$f_{5/2}$	$d_{5/2}$	−0.018	−217.167	3.996
$p_{3/2}$	$d_{3/2}$	0.063	123.146	7.762
$p_{1/2}$	$s_{1/2}$	−0.808	−112.573	90.939
$i_{11/2}$	$h_{11/2}$	0.061	−421.981	−25.884
$g_{9/2}$	$h_{9/2}$	0.004	143.803	0.516
Total				77.676

other single-particle contributions are destructive to $\nu 2p_{1/2} \rightarrow \pi 2s_{1/2}$ and so this is a classic anticoherent state. Nevertheless, the $\nu 2p_{1/2} \rightarrow \pi 2s_{1/2}$ transition is dominate enough so that the $\log f_0 t$ is low. Another example of an anticoherent transition is the neutrino capture by $^{205}\mathrm{Tl}(\frac{1}{2}^+)$ leading to $^{205}\mathrm{Pb}(\frac{1}{2}^-)$.[11] The predictions for such anticoherent transitions are inherently less reliable than those for "coherent" transitions. The $R1$ decays can be understood in the same way, but the remarkable clarity of the effects observed for $R0$ decays is somewhat diminished. The present results provide a further reason in addition to those already known for the plethora of fast first-forbidden β^- decays in the lead region. The observed coherency is quite remarkable. It results in large matrix elements even in those cases where the transitions are not very single-particle-like.

We have made the assumption that ϵ_{MEC} is state independent. Our results would suggest that this assumption is good to within the theoretical uncertainty in ϵ_{MEC}, $\sim 6\%$. The justification for this assumption comes from the studies[3] showing that the MEC enhancement is well approximated by a matrix element proportional to that of $\boldsymbol{\sigma}\cdot\mathbf{p}/M$ which is the nonrelativistic form of γ_5.

The only known calculation of the two-body MEC contribution for the lead region gives[4] $\epsilon_{\mathrm{MEC}}=1.40$ for the $\nu 2p_{1/2} \rightarrow \pi 2s_{1/2}$ transition in $A=206$. This result is in serious disagreement with the present finding of 2.01. Let us discuss the ingredients of this disagreement.

Possible errors in the present calculation.—The success with which the $R1$ moments have been reproduced provides considerable confidence in the calculations. Thus, we are looking for an error(s) in our calculations which is systematic enough to be parametrized successfully and leaves the $R1$ decays essentially unaffected. One possibility has to do with the very large effect of the tensor part of the G matrix on q_S and q_T.[3,19] Because M_0^S and M_0^T are conjugate operators, we have $1-q_T \approx -(1-q_S)$ so that any change in these factors has a magnified effect on $B_1^{(0)}$. The large tensor contribution to the interaction is illustrated by the H7B result for the $\nu 2p_{1/2} \rightarrow \pi 2s_{1/2}$ transition; for it, $q_S = 1 - 0.381 + 0.305$, where the last two terms are the central and tensor contributions, respectively.[19] A 60% tensor reduction, coupled with $\epsilon_{\mathrm{MEC}}=1.4$, would give agreement with experiment. This reduction has the deficiency that it will decrease the agreement for the $R1$ moments.

Relativistic effects.—Kirchbach and Reinhardt[4] noted that the enhancement of 40% was not enough to bring the $R0$ $\log f_0 t$ values for $^{206}\mathrm{Hg} \rightarrow {}^{206}\mathrm{Tl} \rightarrow {}^{206}\mathrm{Pb}$ into agreement with experiment. They proposed relativistic (or other?) effects which could be parametrized by an effective nucleon mass M^* via

$$\gamma_5 \overset{\text{nonrel}}{\rightarrow} \boldsymbol{\sigma}\cdot\mathbf{p}/M^* . \tag{6}$$

The present results would give $M^* \approx 0.7M$ assuming this parametrization to be equally applicable to the one-body and two-body contributions.

In conclusion, the result $\epsilon_{\mathrm{MEC}}=2.01\pm0.05$ is in very poor agreement with the only calculation[4] of the MEC effect in the lead region. This calculation would give $\epsilon_{\mathrm{MEC}} \approx 1.4$ if the enhancement were due to MEC effects alone. Either the calculation[4] is a severe underestimation of the MEC contribution or some other effect is also contributing. There is no obvious explanation for this discrepancy and so one is lead to consider unobvious ones. One possibility is that the tensor contribution to the effective nuclear interaction is seriously overestimated. Kirchbach and Reinhardt suggest the possibility of relativistic effects. Certainly, more theoretical work needs to be done to address these questions.

Research was supported by the U.S. Department of Energy under Contract No. DE-AC02-76CH00016.

[1]K. Kubodera, J. Delorme, and M. Rho, Phys. Rev. Lett. **40**, 755 (1978).

[2]P. Guichon *et al.*, Phys. Lett. **74B**, 15 (1978).

[3]I. S. Towner, Comments Nucl. Part. Phys. **15**, 145 (1986).

[4]M. Kirchbach and M. Reinhardt, Phys. Lett. B **208**, 79 (1988).

[5]D. J. Millener and E. K. Warburton, in *Nuclear Shell Models,* edited by M. Vallieres and B. H. Wildenthal (World-Scientific, Singapore, 1985), p. 365.

[6]E. K. Warburton, in *Interactions and Structures in Nuclei,* edited by R. J. Blin-Stoyle and W. D. Hamilton (Adam Hilger, Bristol, 1988), p. 81.

[7]W. C. Haxton and C. Johnson, Phys. Rev. Lett. **65**, 1325 (1990).

[8]E. K. Warburton *et al.*, Ann. Phys. (N.Y.) **187**, 471 (1988).

[9]H. Mach *et al.*, Phys. Rev. C **41**, 226 (1990).

[10]National Nuclear Data Center on-line retrieval system.

[11]E. K. Warburton (to be published).

[12]B. A. Brown *et al.*, computer code OXBASH, 1984 (unpublished).

[13]N. A. F. M. Poppelier and P. W. M. Glaudemans, Z. Phys. A **329**, 275 (1988).

[14]T. T. S. Kuo and G. H. Herling, U.S. Naval Research Laboratory Report No. 2258, 1971 (unpublished).

[15]E. K. Warburton and B. A. Brown, Phys. Rev. C **43**, 602 (1991).

[16]A. Hosaka *et al.*, Nucl. Phys. **A244**, 76 (1985).

[17]H. Behrens and W. Bühring, *Electron Radial Wave Functions and Nuclear Beta-Decay* (Clarendon, Oxford, 1982).

[18]J. Streets *et al.*, J. Phys. G **8**, 839 (1982).

[19]E. K. Warburton, Phys. Rev. C **42**, 2479 (1990).